International Journal of Minerals, Metallurgy and Materials
Volume 28, Number 4, April 2021, Page 553
https://doi.org/10.1007/s12613-020-2177-y

Invited Review

Effects of heat treatment on the microstructure and mechanical properties of Ni_3Al-based superalloys: A review

Yu-ting Wu, Chong Li, Ye-fan Li, Jing Wu, Xing-chuan Xia, and Yong-chang Liu

State Key Lab of Hydraulic Engineering Simulation and Safety, School of Materials Science & Engineering, Tianjin University, Tianjin 300354, China
(Received: 12 June 2020; revised: 25 August 2020; accepted: 25 August 2020)

Abstract: Ni_3Al-based alloys have drawn much attention as candidates for high-temperature structural materials due to their excellent comprehensive properties. The microstructure and corresponding mechanical properties of Ni_3Al-based alloys are known to be susceptible to heat treatment. Thus, a significant step is to employ various heat treatments to derive the desirable mechanical properties of the alloys. This paper briefly summarizes the recent advances in the microstructure evolution that occurs during the heat treatment of Ni_3Al-based alloys. Aside from γ′ phase and γ phase, the precipitations of β phase, α-Cr precipitates, and carbides are also found in Ni_3Al-based alloys with the addition of various alloying elements. The evolution in morphology, size, and volume fraction of various types of secondary phases during heat treatment are reviewed, involving γ′ phase, β phase, α-Cr precipitate, and carbides. The kinetics of the growth of precipitates are also analyzed. Furthermore, the influences of heat treatment on the mechanical properties of Ni_3Al-based alloys are discussed.

Keywords: intermetallics; heat treatment; microstructure; mechanical properties

1. Introduction

With the development of aerospace technology, the performance of high-temperature structural materials needs to improve because of the constantly increasing thrust-to-weight ratio and the working temperature of the combustion chamber. Intermetallics-based alloys possess a desirable combination of physicochemical and mechanical properties at elevated temperatures because of their stable long-range ordered structure up to a critical temperature [1−7]. As a consequence, the research and development of intermetallic based alloys for high-temperature structural applications have become the focus of researchers. In the past few decades, extensive investigations of intermetallic based alloys have been conducted, and most of them mainly concentrated on Ni−Al, Fe−Al, Ti−Al, and Mo−Si binary systems [8−14]. Among the most investigated of these intermetallics in Ni−Al system is the Ni_3Al-based intermetallic alloys [8,15]. Ni_3Al-based alloys exhibit more appealing properties in comparison to conventional Ni-based alloys, such as high melting point (~1395°C), low density, anomalous temperature dependence of the yield strength, and excellent corrosion resistance [3,16−20].

However, the brittleness of polycrystalline Ni_3Al-based alloys at room temperature makes them difficult to process and fabricate, thereby greatly restricting their structural applications [21−23]. The room-temperature brittleness of polycrystalline Ni_3Al-based alloys is ascribed to the decreased dislocation mobility in highly ordered lattices [23−24]. To further promote wider applications, extensive efforts have been made to improve the intrinsic brittleness of Ni_3Al-based alloys at room temperature. Akoi and Izumi [25] found that a small addition of boron significantly suppresses the embrittlement of Ni_3Al-based alloys. Liu *et al.* [21] studied the effect of boron additions on the grain-boundary chemistry and tensile properties of Ni_3Al-based alloy, and it is found that boron additions can significantly improve the room-temperature ductility of the alloy. George *et al.* [26] indicated that the improvement in the ductility of Ni_3Al-based alloy with boron addition could be primarily associated with its positive impact on suppressing environmental embrittlement. Some researchers found that a small addition of Zr helped ductilize the Ni_3Al-based alloy [27−30]. In addition, Baker [31] presented an effective way to improve the ductility of intermetallics and suggested that the ductility of these intermetallic compounds could be improved if fine hard particles homogenize slip and reduce the lengths of dislocation pile-ups.

Following these findings, numerous studies have been

Corresponding authors: Chong Li E-mail: lichongme@tju.edu.cn; Yong-chang Liu E-mail: ycliu@tju.edu.cn

conducted on the microstructure and mechanical properties of Ni_3Al-based alloys and the relationship between them. The microstructure, including microsegregation, grain size, and characteristics of various precipitates, is a key factor in the mechanical properties of alloys [32−38]. Meanwhile, the microstructure evolution of alloys is considerably governed by the processing parameters during heat treatments. Therefore, the effects of the heat treatment on the microstructure evolution and mechanical properties of Ni_3Al-based alloys need to be clarified to provide reliable experimental and theoretical evidence for microstructure control and further improve the mechanical properties. Many studies have dealt with the developments in the heat treatment of Ni_3Al-based alloys over the past few decades, and most previous studies mainly focused on the solution heat treatment and aging treatment [39−44]. The solution treatment generally results in the dissolution of precipitates and the elimination of microstructural segregation in Ni_3Al-based alloys. The precipitation and growth of precipitates during aging treatment and its influence on mechanical properties were also investigated. In this paper, the various heat treatment processes and the corresponding microstructure evolution during heat treatment of Ni_3Al-based alloys are summarized, and the effects of heat treatment on the mechanical properties are discussed. For organizational purposes, recent advances in research on the heat treatment of Ni_3Al-based alloy can be divided into two sections: solution heat treatment and aging treatment.

2. Phase composition of Ni_3Al-based alloys

Compared with conventional Ni-based alloys, one of the most important characteristics of Ni_3Al-based alloys is their high Al content, which can also be referred to as a low Ni/Al ratio. The microstructure of Ni_3Al-based alloys is mainly γ′ phase and γ phase. Besides, β phase, α-Cr precipitate, and some kinds of carbides are also reported in Ni_3Al-based alloys with various alloying additions.

2.1. γ phase and γ′ phase

The low Ni/Al ratio makes the volume fraction of γ′ phase in Ni_3Al-based alloys higher than that in Ni-based alloys, reaching up to above 80% [45]. The excellent performances of Ni_3Al-based alloys at elevated temperatures are primarily derived from the unique two-phase structure, i.e., the ordered γ′ phase with high volume fraction distributes in the disordered γ matrix. Both the γ′ phase and γ phase exhibit a face-centered cubic (fcc) structure. The Ni solid solution γ phase has an A1 crystal structure (space group: Fm3m). The cubic lattice parameter (a) of γ phase depends on the types and contents of the solid solution elements and varies within a 0.352 to 0.360 nm range [46]. Fig. 1(a) displays the prototype crystallographic structure of γ phase, and the Ni atoms occupy the face centers and corner positions. The γ phases usually distribute around the cuboidal γ′ phases in the form of a net channel in Ni_3Al-based alloys, so it is also referred as γ channel, as shown in Fig. 2. The γ′ phase has a chemical composition of Ni_3Al with $L1_2$ crystal structure (space group: Pm3m), and its prototype crystallographic structure is presented in Fig. 1(b). In the crystal structure of ordered γ′ phase, Ni atom occupies the face centers, while Al atom occupies the corner positions. The lattice parameter (a) of γ′ phase changes from 0.356 to 0.361 nm, which is affected by the addition of alloying elements in alloys [46]. Moreover, the γ′ phase is coherent with the γ matrix, so the γ′ interface energy is relatively small, which ensures homogeneous nucleation of the γ′ phase.

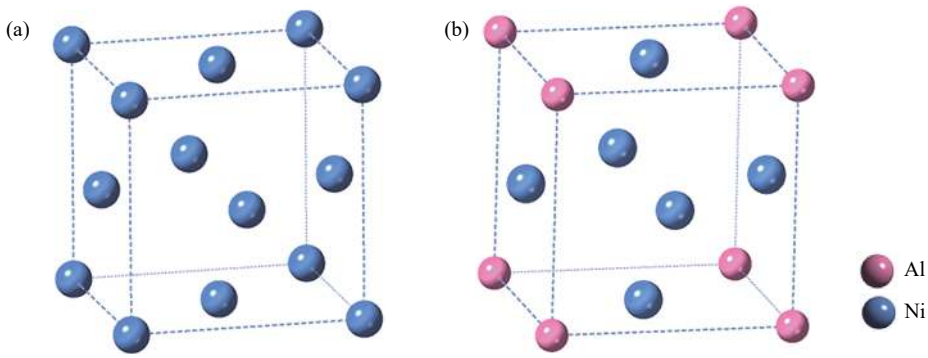

Fig. 1. Crystallographic prototype structure of (a) γ phase and (b) γ′ phase.

2.2. β phase

The β phase has a chemical composition of NiAl with ordered body-centered cubic (bcc) B2 crystal structure (space group: Pm3m), as shown in Fig. 3 [47]. In the crystal structure of β phase, Ni atom occupies the body center, while Al atoms occupy the corner positions. When part of Al atoms is replaced by Ti, Nb, and Hf atoms, the crystal structure of β phase will be further ordered to form a Heusler-type phase (such as Ni_2AlTi phase and Ni_2AlHf phase, denoted as β′), improving the mechanical properties of alloys [48].

Previous research proved that the addition of Fe and Cr

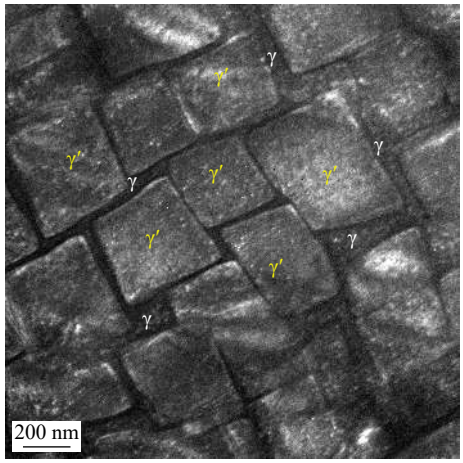

Fig. 2. γ/γ′ microstructure of a cast Ni_3Al-based alloy.

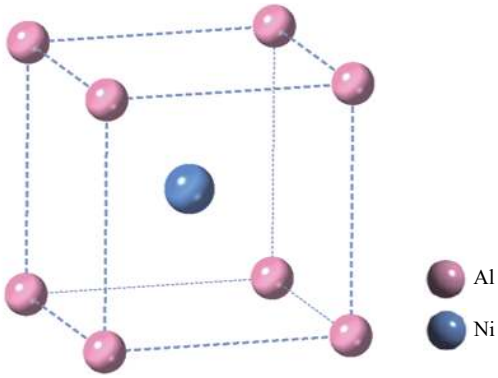

Fig. 3. Crystallographic prototype structure of β phase.

element in Ni_3Al-based alloys mainly promotes the precipitation of β phase, and the Fe atoms will mainly substitute for Ni atoms when the Fe content in Ni_3Al-based alloy exceeds 15at%, leading to the increasing fraction of γ phase in the alloys [45,49]. In addition, the stability of the precipitated β phase is closely related to the Ni/Al ratio. As a result of the wide composition range of the β phase, various phases can also be precipitated in the interior of β phase during heat treatment, such as plate-like γ′ phase and α-Cr, which will be discussed in detail in the next section.

2.3. α-Cr phase

The addition of Cr (up to 8at%) effectively improves the oxidation resistance of Ni_3Al-based alloys by forming a continuous and compact Cr_2O_3 oxide layer on the surface of the alloys [50−51]. Meanwhile, the relatively high addition of Cr gives rise to the precipitation of α-Cr phases with a bcc structure. The α-Cr precipitates have different morphologies in different matrices and exhibit different orientation relationships with the matrices. For instance, the α-Cr precipitates in β phase are spherical and related to the parent phase by a parallel orientation relation, while those in γ′ phase have a lath-shaped morphology and show a Kurdjumov–Sachs orientation relationship with the parent phase [50]. Previous research by Pérez *et al.* [52] found that the volume fraction, size, and distribution of α-Cr precipitates have significant effects on the mechanical properties of a rapidly solidified Ni_3Al−Cr alloy. The extensive precipitation of α-Cr phases during thermal annealing at 750°C results in the embrittlement of the alloy. When the annealing temperature rises to 900 or 1000°C, the α-Cr precipitates tend to re-dissolve in the γ′-Ni_3Al, improving the ductility of alloys.

2.4. Carbides

The main carbides precipitated in the casting Ni_3Al-based alloys include MC and $M_{23}C_6$ (M in MC signifies Hf, Ti, and Zr, while M in $M_{23}C_6$ denotes Cr) [45,53−56]. As shown in Fig. 4, some HfC carbides precipitate in the grain boundaries of the Ni_3Al-based alloys. Different types of carbides can be converted to each other under certain conditions. Moreover, the discontinuously distributed carbides in the grain boundaries can pin the grain boundaries and hinder migration. The brittleness of Ni_3Al-based alloys primarily originates at grain boundaries. Thus, an appropriate amount of carbides can be introduced to strengthen the grain boundaries, reducing the brittleness.

3. Solution heat treatment

The solution heat treatment of alloys is performed at a rel-

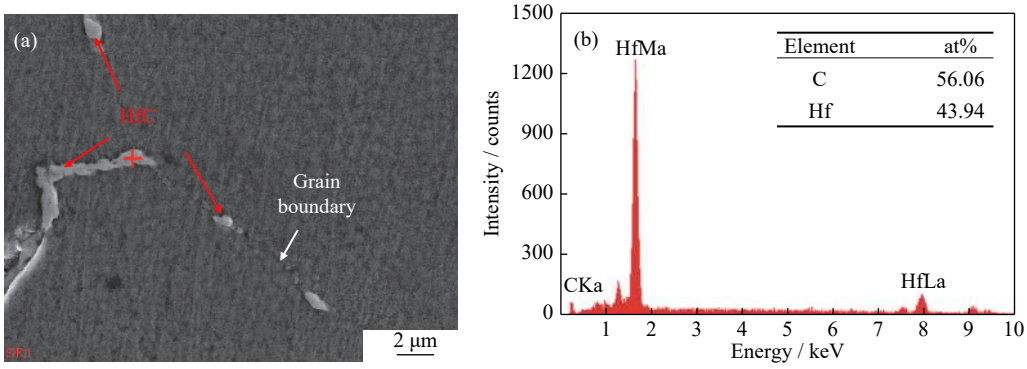

Fig. 4. (a) SEM micrograph of a Ni_3Al-based alloy, showing the appearance of HfC and (b) EDS results of HfC.

atively high temperature to dissolve secondary particles that form during solidification and homogenize the concentration of the alloying elements in solid solution. The dissolution rate of these particles increases with the increasing solution temperature.

3.1. Microstructure evolution

The as-cast microstructure of the Ni_3Al-based alloy is sensitive to the alloy composition. As reported by Zhang *et al.* [57], the as-cast microstructure of Ni_3Al-based alloy MX246 with the composition of Ni−8Al−7Cr−0.6Zr−Ti, B, C is mainly composed of dendrite γ+γ′, eutectic γ-γ′, and Zr-rich phases. They also found that with alloying additions of Mo and Hf, the eutectic γ-γ′ become dispersive, small, and uniform, and its amount is decreased in MX246A with the composition of Ni−8A1−7Cr−2W−4Mo−0.5Hf−Ti, B, C. Wright and Knibloe [58] suggested that the additions of Fe and Cr in Ni_3Al-based alloys with the effectively Al-rich compositions result in the formation of γ, γ′, and martensite β′ phase. Li *et al.* [59] found that the microstructure of Ni_3Al−Fe alloy consists of γ′ and β phases, and it exhibits good ductility. Fig. 5 presents the microstructure of a cast Ni_3Al-based alloy with high Fe content, showing the typical dendritic microstructure. As shown in the higher-magnification SEM image of dendritic regions (Fig. 5(b)), the cuboidal γ′ precipitates embedded in the γ matrix and many fine γ′ precipitates that are as small as nanometer scale are distributed in the γ channel. The average size of the cuboidal γ′ precipitates is 460 nm. Fig. 5(c) shows that an envelope structure with a width of about 1.8 μm exists between the dendritic area and interdendritic area, and the energy dispersive spectrometer (EDS) result of this envelope structure demonstrates that it can be referred as γ′-envelope. On the basis of the microstructure characterizations and the differential scanning calorimetry curves of the as-cast alloys and the correlation phase diagram of the Ni_3Al-based alloy with high Fe content, Wu *et al.* [45] in our research group concluded that the precipitation sequence of the main phases in the experimental Ni_3Al-based alloy during the solidification process is as follows: (a) the dendrite γ phase is first formed from the liquid phase; (b) the interdendritic β phase is formed in the remaining liquid phase, and the rod-shaped Cr_3C_2 phase is precipitated in the β phase; (c) the remaining liquid phase around the β phase forms γ′-envelope structure; (d) the primary γ′ phase precipitates in the dendrite γ phase, and the needle-like γ′ phase precipitates in the β phase; and (e) the secondary γ′ phases precipitate in the γ channel of the dendrite area, and spherical α-Cr phases precipitate in the interdendritic β phase. The as-cast microstructure of alloys is closely associated with the process parameters during solidification. Previous research demonstrated that the cooling rate during the solidification process not only affects the morphology and size of precipitates, dendritic spacing, and solute segregation, but also has an important effect on the precipitation sequence and distribution of precipitates in the matrix of alloys. Ai *et al.* [60] studied the effect of withdrawal rate on the microstruc-

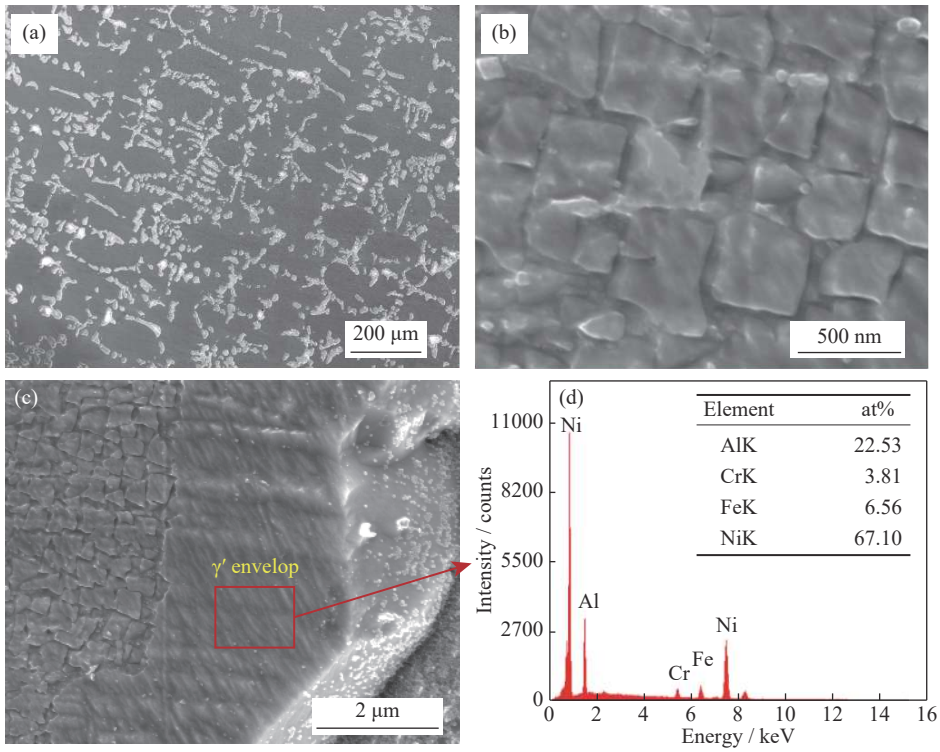

Fig. 5. SEM micrographs of the microstructure of a cast Ni_3Al-based alloy with high Fe content: (a) low magnification, (b) high magnification, (c) morphology of γ′-envelope structure, and (d) EDS result of the envelope structure.

ture and γ/γ′ lattice misfit of a newly developed Re-containing Ni_3Al-based single-crystal (SC) superalloy. The as-cast microstructure changs from planar to cellular and then to dendritic with the increase in the withdrawal rate, and the dendrite and γ′ phases are greatly refined. Moreover, microsegregation inevitably occurs in cast Ni_3Al-based alloys due to the dendritic microstructure. Therefore, the solution heat treatment is needed to reduce the dendritic/interdendritic microsegregation degree and obtain a homogeneous microstructure.

Some studies on the microstructure evolution and corresponding mechanical properties of Ni_3Al-based alloys during solution heat treatment were recently undertaken. Li *et al.* [61] studied the influence of solution treatment on the microstructure and stress rupture properties of a Ni_3Al-based single crystal superalloy IC6SX. They found that the dendritic structure of the experimental alloy disappears and re-precipitated γ′ phases with an average size of about 0.28 μm are distributed homogenously in the matrix after solution treatment at 1280°C, leading to an increase in the stress rupture life. Wang *et al.* [62] reported that the decomposition of carbides and the variation of γ′ phases in the dendritic areas of MX246A alloy occur during the solution treatment. In addition, Ai *et al.* [63] applied a multistep solution treatment to eliminate the precipitation of γ′ phase in interdendritic regions and reduce the microsegregation in a Re-containing Ni_3Al-based SC superalloy. The optimal multistep solution treatment temperature is 1335 to 1355°C for 16 h and followed by air cooling. Lee [43] examined the microstructures of IC221M alloy after solution heat treatment at 1100°C. The γ+Ni_5Zr eutectic colonies are almost eliminated after solution treatment, and the coarsening of γ and γ′ phases are also observed.

In our previous study, a cast Ni_3Al-based alloy was subjected to solution treatment at 1230°C for 16 h to reduce the inhomogeneity of chemical composition and microstructure to some extent. The microstructure of the solution-treated samples is displayed in Fig. 6. After the solution treatment, the interdendritic phase of the experimental Ni_3Al-based alloy is spheroidized, and its volume fraction is slightly decreased. Fig. 6(b) shows that the average size of γ′ precipitates decreased to about 150 nm, and the γ′ precipitates basically still maintain their initial cuboidal morphology. According to a previous study [53], the γ′ solvus temperature of the γ′+γ dendrite areas in the experimental alloy is about 1117°C. Thus, the original coarse γ′ precipitates, which are presented in the as-cast condition, can be inferred to have dissolved completely into the γ matrix during the solution treatment, and then γ′ precipitates are re-precipitated from the supersaturated γ matrix during the subsequent quenching process. In fact, suppressing the re-precipitation of γ′ during quenching after solution treatment is practically impossible. Singh *et al.* [64] suggested that the re-precipitation of γ′ precipitates in alloy 693 can be suppressed only when the cooling rate exceeds 4500°C/min. Moreover, the morphology and size of γ′ precipitates are closely associated with the cooling rate, which will be discussed in the following section. Fig. 6(c) shows that the width of the γ′-envelope also decreases by half after solution treatment. Moreover, parallel lath-shaped substructures are formed in the interdendritic areas of the solution-treated Ni_3Al-based alloy, as indicated by yellow arrows in Fig. 6(c). The formation of lath-shaped structures may be ascribed to the non-uniform plastic deformation of dendrite and interdendrite area during heat treatment. Another account suggests that the formation of lath-shaped structures is related to the martensite phase transformation of β phase during the rapid cooling process. In actual, the formation mechanism of lath-structure of β phase has not yet been clearly stated so far and needs to be further studied in future works. Li *et al.* [65] observed similar lath-shaped structures in the interdendrite β phase of a rapidly solidified Ni_3Al-based alloy, as displayed in Fig. 7. Rapid solidification rate would result in the massive precipitation of α-Cr precipitates, which promotes the transformation from β phase with B2 structure to martensite phases with a $L1_0$ structure, forming a high density of stacking faults and microtwins in interdendritic areas. The selected area electron diffraction (SAED) pattern of the lath-shaped structures is shown in Fig. 7(b), revealing the characteristic of twins. The microstructure evolution of the interdendritic areas in a Ni_3Al-based alloy during solution treatment was also investigated in our previous research [66], and findings show that the formation of precipitates in inter-

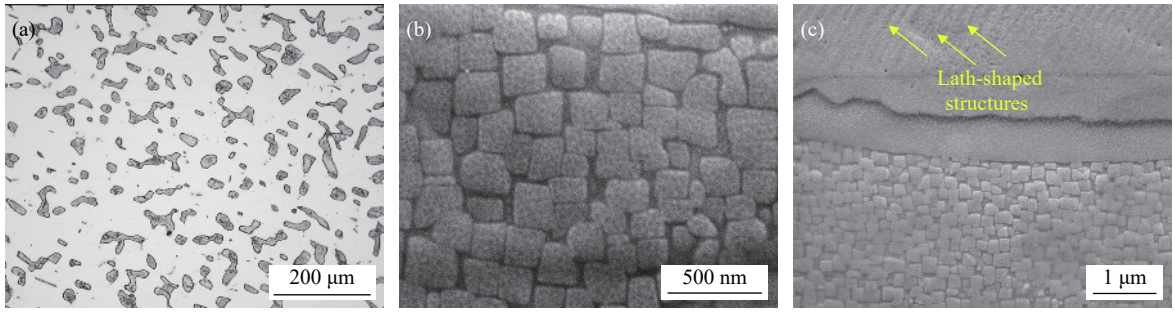

Fig. 6. Microstructure of a Ni_3Al-based alloy after solution treatment at 1230°C for 16 h and followed by air cooling: (a) low-magnification optical micrograph and high-magnification morphology of (b) the γ′+γ dendrite and (c) the γ′-envelope structure.

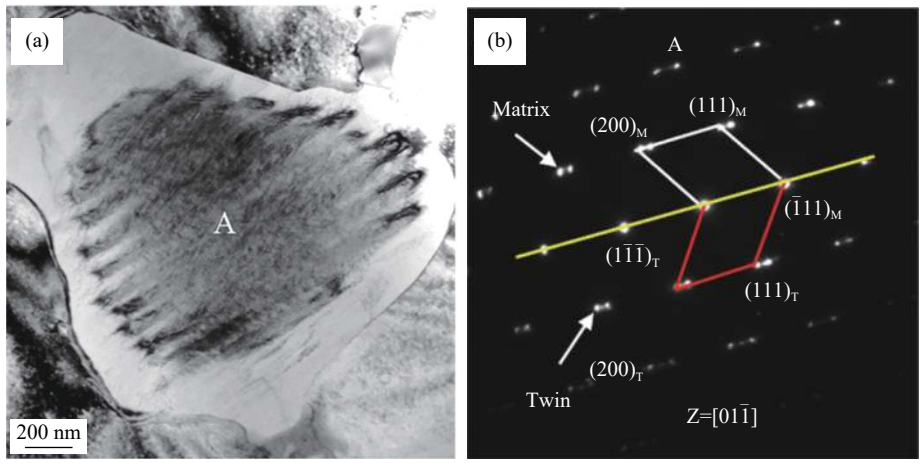

Fig. 7. (a) TEM morphology of the interdendritic region of a spray-casting Ni_3Al-based alloy and (b) the SAED pattern of region A in (a). Reprinted from *Mater. Lett.*, 250, Y.F. Li, C. Li, J. Wu, Y.T. Wu, Z.Q. Ma, L.M. Yu, H.J. Li, and Y.C. Liu, Formation of multiply twinned martensite plates in rapidly solidified Ni_3Al-based superalloys, 147-150, Copyright 2019, with permission from Elsevier.

dendritic areas depends strongly on the cooling rates, which will be discussed in the next section.

3.2. Quenching sensitivity

The main aim of quenching is to control the precipitation of the alloys during the cooling process, further obtaining desirable performance. In general, the cooling rate has a significant impact on the precipitation in alloys, including morphology, size, distribution, and variety [66−68]. When the cooling rate is sufficiently high, solute will be retained in the solid solution and the precipitation will be suppressed. In contrast, if the cooling rate is relatively slow, then precipitation will occur at grain boundaries, dislocations, or other defects, which gives rise to lower supersaturation of solute.

To clarify the effect of solution cooling rate on the microstructure evolution of a multiphase Ni_3Al-based alloy, different cooling methods, i.e., water cooling (WC), air cooling (AC), and furnace cooling (FC), were applied after solution treatment at 1200°C for 10 h in our previous study [66]. The cubic degree, size, and volume fraction of primary γ′ precipitates in the γ′+γ dendrite decreases as the cooling rates increases, and the average size of secondary γ′ precipitates increases as well. The influence of cooling rate on the size and volume fraction of primary and secondary γ′ precipitates in γ′+γ dendrite of the experimental alloy is summarized in Fig. 8. A logarithmic relationship is found between the average size of γ′ phase and the cooling rates, whether for primary γ′ or secondary γ′. The logarithmic relationships are calculated as $\lg D_{\gamma'} = 2.4128 - 0.3266 \times \lg(\mathrm{d}T/\mathrm{d}t)$ and $\lg D_{\gamma'} = 0.6353 - 0.7430 \times \lg(\mathrm{d}T/\mathrm{d}t)$ for primary γ′ and secondary γ′, respectively, where $D_{\gamma'}$ is the average size of the primary or secondary γ′ phase, and $\mathrm{d}T/\mathrm{d}t$ presents the cooling rate. According to the examination of the interdendritic microstructure, the precipitation of semi-spherical α-Cr particles and long acicular γ′ precipitates can be promoted with the decreasing cooling rate, while the number of rod-like Cr_3C_2 carbides decreases, as illustrated in Fig. 9. Parallel lath-shaped structures are also found in the interdendritic areas of WC and AC samples, thereby indicating that the width of the parallel lath-shaped structures decreases as the cooling rate decreases. From Fig. 9, we can conclude that the formation of parallel lath-shaped structures is sensitive to the cooling rate. The high thermal stress caused by rapid cooling rate would lead to plastic deformation in the local area of the alloy. The cooling rate can also significantly influence the precipitates in the interdendritic areas of Ni_3Al-based alloy. Different cooling rates lead to the formation of three kinds of precipitates in the interdendritic area, namely, rod-like Cr_3C_2 carbides, semi-spherical α-Cr particles, and long acicular γ′ precipitates [66]. The thermal stability of these precipitates

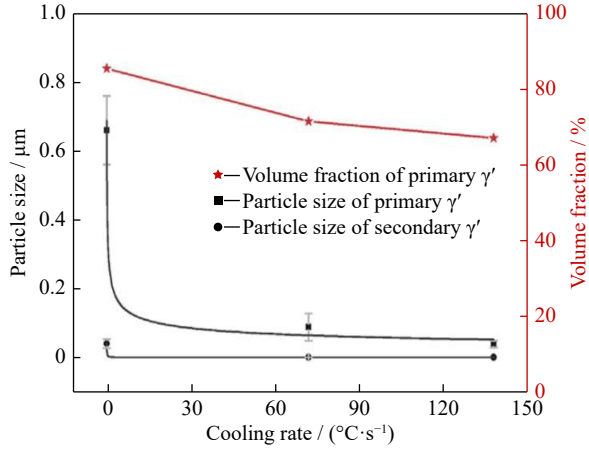

Fig. 8. Size and volume fraction of primary and secondary γ′ precipitates in γ′+γ dendrite of Ni_3Al-based alloy after solution treatment as a function of cooling rate. Reprinted from *Intermetallics*, 109, J. Wu, C. Li, Y.C. Liu, X.C. Xia, Y.T. Wu, Z.Q. Ma, and H.P. Wang, Influences of solution cooling rate on microstructural evolution of a multiphase Ni_3Al-based intermetallic alloy, 48-59, Copyright 2019, with permission from Elsevier.

varies decreasingly in the following sequence: acicular γ′ precipitates > semi-spherical α-Cr particles > rod-like Cr_3C_2 carbides. Consequently, as the cooling rate decreases, the amount of rod-like Cr_3C_2 carbides decreases, whereas that of both the semi-spherical α-Cr particles and long acicular γ′ precipitates increase.

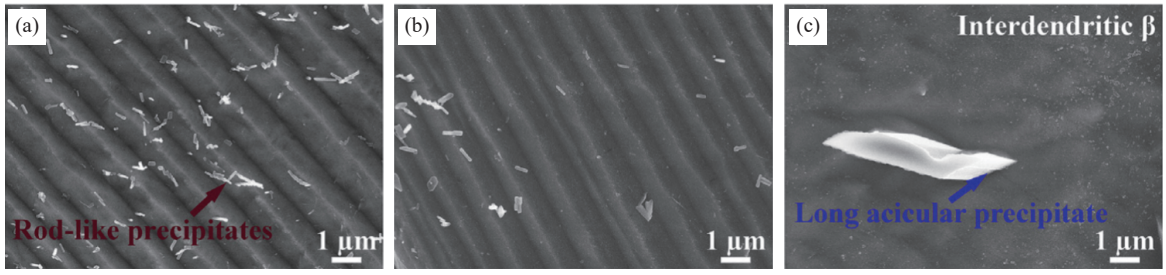

Fig. 9. SEM morphologies of the interdendritic areas in Ni_3Al-based alloy subjected to 1200°C/10 h solution treatment and cooled by (a) WC, (b) AC, and (c) FC. Reprinted from *Intermetallics*, 109, J. Wu, C. Li, Y.C. Liu, X.C. Xia, Y.T. Wu, Z.Q. Ma, and H.P. Wang, Influences of solution cooling rate on microstructural evolution of a multiphase Ni_3Al-based intermetallic alloy, 48-59, Copyright 2019, with permission from Elsevier.

From the above, we can conclude that the microstructure of Ni_3Al-based alloys is sensitive to the solution cooling rates. The cooling rate during solidification process is also a key factor in determining the microstructure of alloys, which has an important influence on the type, quantity, and distribution of precipitates. Li *et al.* [69−70] investigated the effects of solidification rate on the microstructure evolution and phase transition mechanism of a polycrystalline Ni_3Al-based alloy with high Fe and Cr contents. The microstructures of the alloy with different solidification rates all exhibit typical characteristics of dendritic microstructure. The volume fraction of interdendritic areas increases with the increase in solidification rate, while the secondary dendrite spacing decreases. Rapid solidification cooling rate (~10^3 K/s) directly changes the size of the γ′ phase in the dendritic areas of the alloy from a bimodal distribution (conventional solidification cooling rate ~10 K/s) to a unimodal distribution, and secondary γ′ phases disappear.

3.3. Effects of solution heat treatment on mechanical properties of alloys

To date, few studies concerning the effect of solution heat treatment of Ni_3Al-based alloys on mechanical properties have been performed. Lee [43] attempted to improve the mechanical properties of a cast Ni_3Al-based alloy by solution heat treatment at 1100°C. The microhardness of the solution-treated alloy is significantly higher than that of the alloy without solution treatment. A solid solution strengthening effect by Zr element due to the dissolution of γ + Ni_5Zr eutectic colonies during the solution treatment is probably responsible for the improvement in hardness. Meanwhile, tensile tests showed that the solution treatment has no evident influence on the tensile properties of alloys. In the investigations of Li *et al.* [61], the stress rupture lives of Ni_3Al-based alloy IC6SX before and after solution heat treatment at different temperatures under the condition of 1100°C/130 MPa were examined to elucidate the influence of solution heat treatment on the stress rupture properties. As presented in Fig. 10, the stress rupture lives of solution-treated specimens are superior to those of the as-cast alloy, which may be due to the minimal variation in the size of the fine re-precipitated γ′ particles. Duan *et al.* [71] studied the effect of solution treatment on the high-temperature tensile properties of a wrought Ni_3Al-based alloy. The results showed that the volume fraction of β phase decreases when the alloy is solution treated at 1280°C, leading to a reduced probability of generating cracks, and both the volume fraction of γ′+γ areas and grain size increase, which results in the improved high-temperature strength of alloy. Hadi and Kamali [72] investigated the influences of solution treatment on hot workability and mechanical properties of Ni_3Al-based IC221M alloy. They found that the solution-treated alloy presents higher hot workability than the as-cast alloy due to the reduction of eu-

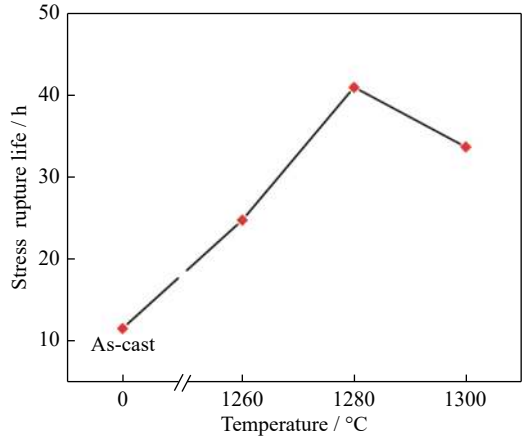

Fig. 10. Effect of solution heat treatment on the stress rupture life of alloy IC6SX under the testing condition of 1100°C/130 MPa. The data used in this graph is obtained from Ref. [61].

tectic phase after solution treatment, and the yield strength of the solution-treated alloy is also higher than that of the as-cast alloy at a testing temperature above 700°C. The results of room temperature tensile tests revealed that the tensile yield strength, ultimate strength, and elongation of the solution-treated alloy are lower than those of as-cast alloy.

4. Aging treatment

The size, morphology, and volume fraction of γ′ phase are widely accepted to be able to greatly affect the mechanical properties of γ′-strengthened superalloys [73−77]. As documented in previous studies on some Ni-based superalloys, at a high volume fraction and cubic degree of γ′ phase, and at a γ′ phase close to 0.45 μm, the creep rupture properties of alloys improve [53,78]. As mentioned above, the average size of γ′ phase in the Ni_3Al-based alloys decreases to a small level after solution treatment, and the cubic degree of γ′ phase is also reduced. Hence, aging treatment is necessary to obtain the cubic γ′ phases with ideal characteristics and achieve optimal mechanical properties. In addition, Ni_3Al-based alloys are expected to be used as high-temperature components exposed to high temperatures in the long term. The service life of those components is directly determined by the variation in microstructure and mechanical properties during thermal exposure. Thus, research on the effect of aging on microstructure and mechanical properties has guiding significance for practical applications.

4.1. Microstructure evolution

Extensive studies about the effects of aging on the microstructure evolution have been conducted in Ni_3Al-based alloys. Lapin [42] revealed that aging in the temperature range from 1023 to 1223 K leads to the transformation from the unstable lamellar γ/γ′-β type structure to γ/γ′-α type structure in a directionally solidified (DS) Ni_3Al-based alloy, and aging at 1123 and 1173 K is the most effective in transforming the unstable lamellae to γ′-phase and α-Cr precipitates. Pérez *et al.* [52] noticed that a large number of α-Cr phases precipitate in a rapidly solidified Ni_3Al–Cr alloy during aging at 750°C, which tend to dissolve after aging at higher temperatures (900 and 1000°C). Wu *et al.* [79] observed that the intersected plate-like γ′ phases precipitate in the interdendritic β phases of a multiphase Ni_3Al-based alloy during long-term aging at 800°C. The precipitation of intersected plate-like γ′ phases was also reported in as-cast and spray casting Ni_3Al-based superalloy during thermal exposure at 600°C by Li *et al.* [69]. Moreover, according to their research, the γ′ precipitates in the dendritic areas of the two states alloys coarsen during exposure at the temperature range from 600 to 900°C, and the morphology of γ′ precipitates varies from cuboidal to irregular shapes, which can be attributed to the coalescence of neighboring particles and Ostwald ripening. Lee *et al.* [80] investigated the thermal aging effects on the microstructure of a castable Ni_3Al-based IC221M alloy. They found that the homogenization of the microstructure is promoted by the thermal aging, and the volume fraction of the γ+Ni_5Zr eutectic is halved after aging at 900°C for 1000 h. With further aging up to 16600 h, the spheroidization of the eutectic colonies occurs, while the volume fraction of the eutectic remains constant. In the as-cast Ni_3Al-based superalloy, the metastable primary carbides are prone to transformation or dissolution upon thermal aging, resulting in the formation of secondary carbides. These tiny secondary carbides are mainly discontinuously distributed in the low-angle grain boundaries or the dendritic areas, which can prevent grain boundary sliding and crack propagation, and the rupture ductility and rupture life of alloys are improved [81−82]. Fig. 11 illustrates the microstructure of an as-cast Ni_3Al-based superalloy after thermal exposure at 600°C for 4 h, showing the morphologies of carbides along the γ′-envelope. Many carbides distribute along the interfaces between the γ′+γ dendritic and γ′-envelope, and these carbides are proved to be $Cr_{23}C_6$ by EDS analysis.

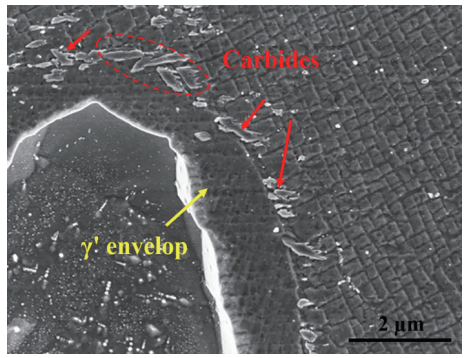

Fig. 11. Microstructure of an as-cast Ni_3Al-based superalloy after thermal exposure at 600°C for 4 h, showing the morphologies of carbides along the γ′-envelope.

In addition to the precipitation of secondary phases and the dissolution and transformation of unstable precipitates, the growth of precipitates by diffusion of atoms from the supersaturated solid solution to the precipitates was reported in previous studies [83−88]. The evolution in microstructure characteristics (such as morphology, size, and distribution) of γ′ precipitates during thermal aging has recently received much attention due to the high volume fraction of γ′ precipitates in Ni_3Al-based alloys. Lee [84] found that the coarsening of γ′ phases in a cast IC221M alloy occurs upon aging at 900°C, which is ascribed to the coalescence of adjacent particles. A similar phenomenon was reported by Li *et al.* [89], who found that the γ′ phases coarsen and connect with each other during long-term aging of a Ni_3Al-based single crystal alloy IC6SX at 1070°C. Motejadded *et al.* [86] examined the morphological evolution and coarsening kinetics of γ′ precipitates in the dendrite regions of IC221M alloy

annealed at 900, 1000, and 1100°C up to 50 h. The annealing treatment leads to the coarsening of γ′ precipitates, and the coarsening process is in accordance with Lifshitz–Slyozov–Wagner (LSW) theory. The coarsening activation energy was calculated as 253.5 kJ/mol, implying that the coarsening of the γ′ precipitates is controlled by the volume diffusion of Al. Wu *et al.* [90] discussed the widening behavior of the γ′-envelope structure in an as-cast multiphase Ni_3Al-based alloy during long-term aging. They concluded that the γ′-envelope widening is primarily controlled by the diffusion of Ni, Al, Hf, and Mo atoms at the γ′+γ /γ′-envelope/β interfaces during the aging process, which involves a relevant phase transformation: β(NiAl) + γ(Ni) → γ′(Ni_3Al). In our previous studies [91], the microstructure evolution in the γ′+γ area of a newly developed Ni_3Al-based alloy during aging at a temperature range from 800 to 1000°C was also studied. The results revealed that the γ′ precipitates coarsen during thermal aging and the morphology of γ′ precipitate changes from cuboidal to strip-like and L-shaped due to the coalescence of adjacent particles, as shown in Fig. 12. The coarsening kinetics of γ′ precipitates was also investigated. The measured temporal evolution of the average size of γ′ precipitates suggested that the process of γ′ precipitate coarsening can be divided into two stages, namely, early stage and later stage, which follow the cube rate law of the Lifshitz–Slyozov encounter modified model and the square rate law of trans-interface diffusion-controlled coarsening model, respectively.

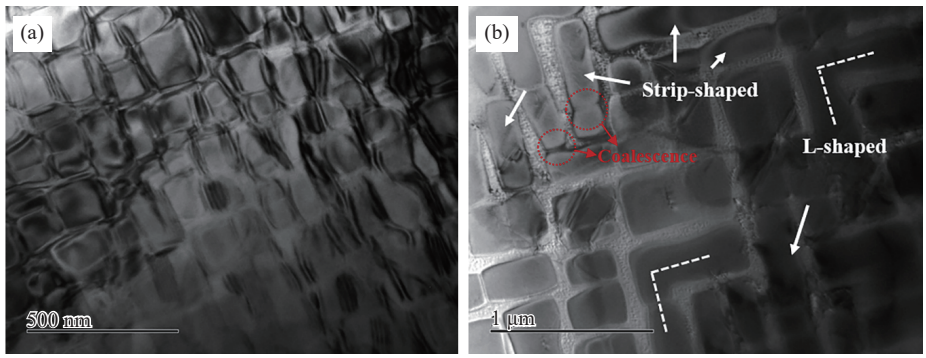

Fig. 12. **γ′+γ microstructures of a Ni_3Al-based alloy after (a) solution treatment and (b) aging at 1000°C for 5 h.**

The changes in other precipitates during aging were also investigated. Lapin and Vaňo [92] found that the α-Cr and γ′ precipitates in dendrites of a multiphase intermetallic Ni–Al–Cr–Ti alloy simultaneously grow during aging at 950–1050°C. The growth of α-Cr precipitates follows LSW theory ($d^3 \propto t$, where d is the mean particle size and t is the aging time), and the activation energy for coarsening is 310 kJ/mol, indicating that the growth of α-Cr precipitates is controlled by volume diffusion of Cr. Meanwhile, the growth of γ′ precipitates follows $d^4 \propto t$ law with the coarsening activation energy of 250 kJ/mol, which suggests that the growth of γ′ precipitates is controlled by diffusion of Ni along the β/γ′ phase boundaries.

4.2. Effect of aging treatment on the mechanical properties

The above findings lead us to think that the aging treatment of the alloys, which have a significant impact on the microstructure, may also inevitably influence its mechanical properties. Lapin *et al.* [93] reported that the hardness of a directionally solidified intermetallic Ni–Al–Cr–Ti alloy is greatly increased after aging at 973 K, while the room-temperature tensile ductility is reduced. Lee and Santella [94] investigated the thermal aging effects on the tensile properties of a Ni_3Al-based alloy. They noticed that the room temperature yield strength decreases with increasing aging time either in air or Ar at 900°C. For aging at 1050 and 1100°C, the room temperature yield strength of the alloy aged in air is significantly reduced, whereas that of the alloy aged in Ar increases. The increase in yield strength in the alloy aged in Ar is attributed to the increasing amount of fine γ′ precipitation in the matrix after aging. Wu *et al.* [90] examined the effects of the widening of the γ′-envelope structure on the creep behavior of a Ni_3Al-based alloy during long-term aging. Fig. 13 shows that the widening of the γ′-envelope occurs during aging, leading to the decrease in the interdendritic β phase and increase in the γ′ phase, which reduces the steady-state creep rate and improves the creep rupture life under the uniaxial constant load tensile creep tests at 800°C/220 MPa. In contrast, a negative response of the mechanical properties to aging was reported by Han *et al.* [95] for a DS casting Ni_3Al-based alloy IC6. The tensile and stress rupture properties of the experimental alloys slowly deteriorate with aging time. This negative response to aging is attributed to the microstructure changes during aging, including the reduction of γ phase, the coalescence and growth of γ′ phase, and the homogenization of alloy element distribution.

In our previous work [96], different initial microstructures were obtained by heat treating the Ni_3Al-based alloy in different ways (i.e., homogenization treatment and aging treat-

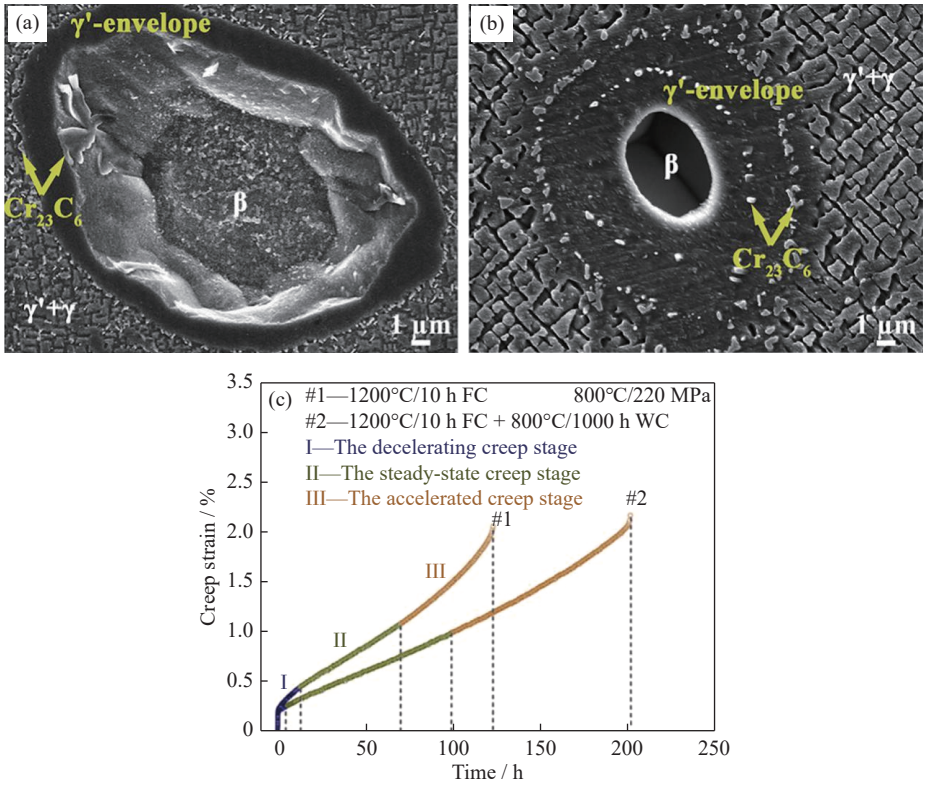

Fig. 13. SEM morphologies of the γ′-envelope structure of a multiphase Ni_3Al-based alloy after (a) annealing at 1200°C for 10 h, (b) annealing followed by aging at 800°C for 1000 h, and (c) the creep curves of the heat-treated samples under 800°C/220 MPa. Reprinted from *Mater. Sci. Eng. A*, 763, J. Wu, C. Li, Y.C. Liu, X.C. Xia, Y.T. Wu, Y.F. Li, and H.P. Wang, Formation and widening mechanisms of envelope structure and its effect on creep behavior of a multiphase Ni_3Al-based intermetallic alloy, 138158, Copyright 2019, with permission from Elsevier.

ment). Thereafter, a comparative study of hot deformation behavior for the Ni_3Al-based alloys was conducted to clarify the effects of initial microstructure on the hot deformation characteristics and deformed microstructure, as shown in Fig. 14. The results revealed that the peak stress and the magnitude of the stress drop for the aged alloy, which presents coarse γ′ precipitates, are higher than those for the unaged alloy with fine γ′ precipitates at a given temperature and strain rate. The critical conditions for dynamic recrystallization of experimental alloys were also determined, and the results showed that critical stress and strain for the aged alloy are higher than those for the unaged alloy. The serration of the flow curves can be also found in Fig. 14(c), especially for the homogenization plus aging sample and relatively high strain rates. The serration of the flow curves could be attributed to an alternation between the work hardening effect and the dynamic softening effect during deformation. In the homogenization plus aging sample, the rapid dislocation accumulation is caused by the coarse strip-like γ′ precipitates, which acts as strong obstacles to the dislocation movement. The increased strain rate is also beneficial to accelerating the dislocation accumulation. Hence, the alternation between the work hardening effect and the dynamic softening effect occurs more frequently, leading to the more apparent serration of the flow curves.

5. Concluding remarks

Ni_3Al-based alloys have attracted much attention as candidates for advanced high-temperature structural materials because of their excellent physical and mechanical properties. Apart from the effects of composition design, solidification, and thermomechanical process, the microstructure and comprehensive properties of alloys are greatly affected by heat treatments. In other words, various heat treatments, including solution heat treatment and aging, have been enforced on Ni_3Al-based alloys to obtain different microstructure and corresponding properties. This paper presents an overview of the effects of heat treatment on the microstructural changes and mechanical properties of Ni_3Al-based alloys, which could be of practical significance for guiding the improvement in properties and predicting the service life of such materials.

Ni_3Al-based alloys mainly consist of γ′ phase and γ phase. Besides, β phase, α-Cr precipitate, and carbides are also found in alloys with various additions of alloying elements. The dissolution of γ′ precipitates and carbides occurs during the solution heat treatment of Ni_3Al-based alloys, which al-

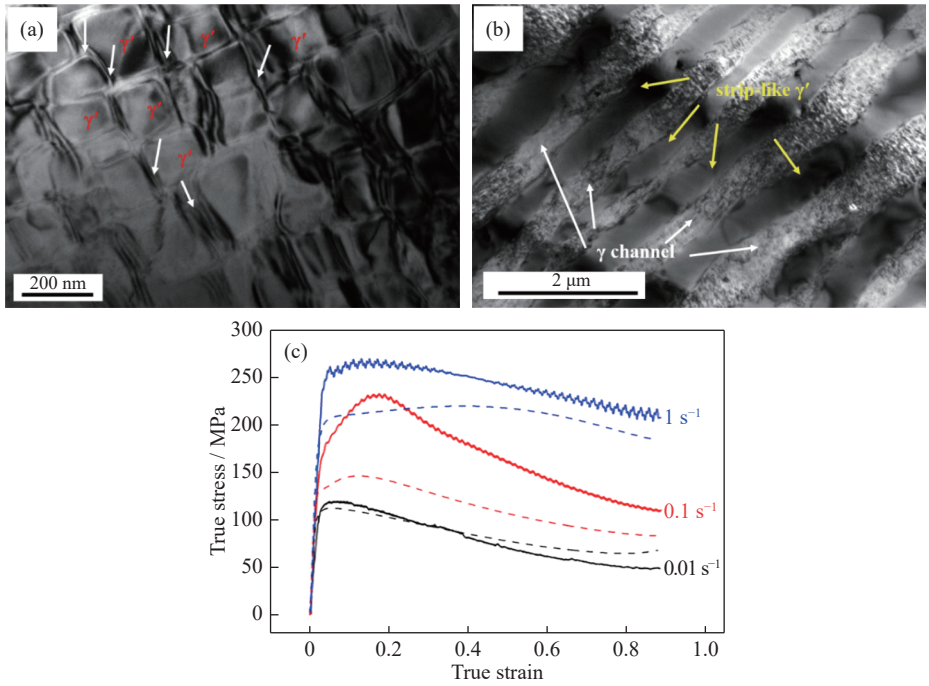

Fig. 14. TEM micrographs of the Ni3Al-based alloy after (a) homogenization, (b) homogenization plus aging, and (c) the flow curves of the alloy deformed at 1100°C with different strain rates, in which dotted lines and solid lines represent the studied alloy after homogenization and homogenization plus aging, respectively. Reprinted from *Intermetallics*, 113, Y.T. Wu, Y.C. Liu, C. Li, X.C. Xia, J. Wu, and H.J. Li, Effect of initial microstructure on the hot deformation behavior of a Ni_3Al-based alloy, 1306584, Copyright 2019, with permission from Elsevier.

lows these phases to optimally re-precipitate in the matrix during the cooling process or subsequent aging treatment for obtaining desirable properties. Suppressing the re-precipitation of γ′ during quenching after solution treatment is also practically impossible. During the cooling process, the microstructure of Ni_3Al-based alloys is sensitive to the cooling rate. Typically, the slower cooling rate causes a higher volume fraction and bigger size of primary and secondary γ′ precipitates, and the α-Cr particles and long acicular γ′ precipitates in the interdendritic areas can also be promoted. The relationship between the mechanical properties and the cooling rate is complicated and experimental data for Ni_3Al-based alloys are lacking, thereby indicating the need for further investigations regarding the effect of cooling rate on the mechanical properties. Recent progress in the influence of aging on the microstructure and properties has been summarized. The precipitation of secondary phases can be promoted during aging, and the dissolution and transformation of unstable precipitates occur at a relatively high aging temperature. Meanwhile, the growth of γ′ precipitates by diffusion of atoms can also be found. Variations in microstructure during aging evidently result in a positive or negative response to the mechanical properties of alloys. The specific impact of aging treatment is affected by the alloying composition, initial microstructure, and aging parameters, which needs to be studied further in future works.

Acknowledgements

This work was financially supported by the National Natural Science Foundation of China (Nos. 52075373 and 52034004) and the National High Technology Research and Development Program of China (No. 2015AA042504).

References

[1] C.T. Liu, and J.O. Stiegler, Ductile ordered intermetallic alloys, *Science*, 226(1984), No. 4675, p. 636.

[2] R. Kozubski, Long-range order kinetics in Ni_3Al-based intermetallic compounds with L12-type superstructure, *Prog. Mater. Sci.*, 41(1997), No. 1-2, p. 1.

[3] P. Jozwik, W. Polkowski, and Z. Bojar, Applications of Ni_3Al based intermetallic alloys—Current stage and potential perceptivities, *Materials*, 8(2015), No. 5, p. 2537.

[4] Y.T. Wu, Y.C. Liu, C. Li, X.C. Xia, Y. Huang, H.J. Li, and H.P. Wang, Deformation behavior and processing maps of Ni_3Al-based superalloy during isothermal hot compression, *J. Alloys Compd.*, 712(2017), p. 687.

[5] S.A. David and S.C. Deevi, Welding of unique and advanced ductile intermetallic alloys for high-temperature applications, *Sci. Technol. Weld. Joining*, 22(2017), No. 8, p. 681.

[6] G. Karin, H.L. Luo, D. Feng, and C.H. Li, Ni_3Al-based intermetallic alloys as a new type of high-temperature and wear-resistant materials, *J. Iron Steel Res. Int.*, 14(2007), No. 5, p. 21.

[7] Y.T. Wu, C. Li, X.C. Xia, H.Y. Liang, Q.Q. Qi, and Y.C. Liu, Precipitate coarsening and its effects on the hot deformation behavior of the recently-strengthened superalloys, *J. Mater. Sci.*

Technol., 67(2021), p. 95.
[8] V.K. Sikka, S.C. Deevi, S. Viswanathan, R.W. Swindeman, and M.L. Santella, Advances in processing of Ni_3Al-based intermetallics and applications, *Intermetallics*, 8(2000), No. 9-11, p. 1329.
[9] M. Yamaguchi, H. Inui, and K. Ito, High-temperature structural intermetallics, *Acta Mater.*, 48(2000), No. 1, p. 307.
[10] N.S. Stoloff, C.T. Liu, and S.C. Deevi, Emerging applications of intermetallics, *Intermetallics*, 8(2000), No. 9-11, p. 1313.
[11] M.H. Enayati and M. Salehi, Formation mechanism of Fe_3Al and FeAl intermetallic compounds during mechanical alloying, *J. Mater. Sci.*, 40(2005), No. 15, p. 3933.
[12] J.H. Schneibel, P.F. Tortorelli, R.O. Ritchie, and J.J. Kruzic, Optimization of Mo–Si–B Intermetallics, *Metall. Mater. Trans. A*, 36(2005), No. 3, p. 525.
[13] J.Y. Guo, Y.F. Li, C. Li, L.M. Yu, H.J. Li, Z.M. Wang, and Y.C. Liu, Isothermal oxidation behavior of micro-regions in multiphase Ni_3Al-based superalloys, *Mater. Charact.*, 171(2021), art. No. 110748.
[14] L.J. Duan and Y.C. Liu, Relationships between elastic constants and EAM/FS potential functions for cubic crystals, *Acta Metall. Sin.*, 56(2020), No. 1, p. 112.
[15] W. Polkowski, P. Jóźwik, K. Karczewski, and Z. Bojar, Evolution of crystallographic texture and strain in a fine-grained Ni_3Al (Zr, B) intermetallic alloy during cold rolling, *Arch. Civ. Mech. Eng.*, 14(2014), No. 4, p. 550.
[16] J.L. Pei, Y.F. Li, C. Li, Z.M. Wang, Y.C. Liu, and H.J. Li, Microstructure-dependent oxidation behavior of Ni-Al single-crystal alloys, *J. Mater. Sci. Technol.*, 52(2020), p. 162.
[17] S.C. Deevi and V.K. Sikka, Nickel and iron aluminides: An overview on properties, processing, and applications, *Intermetallics*, 4(1996), No. 5, p. 357.
[18] L.Y. Sheng, W. Zhang, J.T. Guo, Z.S. Wang, V.E. Ovcharenko, L.Z. Zhou, and H.Q. Ye, Microstructure and mechanical properties of Ni_3Al fabricated by thermal explosion and hot extrusion, *Intermetallics*, 17(2009), No. 7, p. 572.
[19] J.G. Yu, Q.X. Zhang, and Z.F. Yue, Tensile mechanical properties of Ni_3Al nanowires at intermediate temperature, *RSC Adv.*, 4(2014), No. 40, art. No. 20789.
[20] S.V. Raju, B.K. Godwal, A.K. Singh, R. Jeanloz, and S.K. Saxena, High-pressure strengths of Ni_3Al and Ni−Al−Cr, *J. Alloys Compd.*, 741(2018), p. 642.
[21] C.T. Liu, C.L. White, and J.A. Horton, Effect of boron on grain-boundaries in Ni_3Al, *Acta Metall.*, 33(1985), No. 2, p. 213.
[22] H.B. Motejadded, M. Soltanieh, and S. Rastegari, An investigation about the effect of annealing conditions on microstructure in a Ni_3Al base alloy, *J. Alloys Compd.*, 486(2009), No. 1-2, p. 881.
[23] J.S. Wang, Dislocation nucleation and the intrinsic fracture behavior of L12 intermetallic alloys, *Acta Mater.*, 46(1998), No. 8, p. 2663.
[24] S.K. Shee, S.K. Pradhan, and M. De, Effect of alloying on the microstructure and mechanical properties of Ni_3Al, *J. Alloys Compd.*, 265(1998), No. 1-2, p. 249.
[25] K. Aoki and O. Izumi, On the ductility of the intermetallic compound Ni_3Al, *Trans. Jpn. Inst. Met.*, 19(1978), No. 4, p. 203.
[26] E.P. George, C.T. Liu, H. Lin, and D.P. Pope, Environmental embrittlement and other causes of brittle grain boundary fracture in Ni_3Al, *Mater. Sci. Eng. A*, 192-193(1995), p. 277.
[27] Y.F. Gu, D.L. Lin, T.L. Lin, and J.T. Guo, Ductilization of Ni_3Al by alloying with zirconium, *Scripta Mater.*, 35(1996), No. 5, p. 609.
[28] E.P. George, C.T. Liu, and D.P. Pope, Environmental embrittlement: The major cause of room-temperature brittleness in polycrystalline Ni_3Al, *Scripta Metall. Mater.*, 27(1992), No. 3, p. 365.
[29] J.T. Guo, H. Li, and C. Sun, Effect of Zr, Cr and B addictives on microstructure and mechanical properties of Ni_3Al alloys, *Acta Metall. Sin. Engl. Ed.*, 3(1990), No. 3, p. 170.
[30] Y.F. Li, J.T. Guo, L.Z. Zhou, and H.Q. Ye, Effect of recrystallization on room-temperature mechanical properties of Zr-doped Ni_3Al alloy, *Mater. Lett.*, 58(2004), No. 12-13, p. 1853.
[31] I. Baker, Improving the ductility of intermetallic compounds by particle-induced slip homogenization, *Scripta Mater.*, 41(1999), No. 4, p. 409.
[32] E.M. Schulson, T.P. Weihs, D.V. Viens, and I. Baker, The effect of grain size on the yield strength of Ni_3Al, *Acta Metall.*, 33(1985), No. 9, p. 1587.
[33] M. Takeyama and C.T. Liu, Effect of grain size on yield strength of Ni_3Al and other alloys, *J. Mater. Res.*, 3(1988), No. 4, p. 665.
[34] P. Jóźwik and Z. Bojar, Analysis of grain size effect on tensile properties of Ni_3Al based intermetallic strips, *Arch. Metall. Mater.*, 52(2007), No. 2, p. 321.
[35] X. Zhang, H.W. Li, M. Zhan, Z.B. Zheng, J. Gao, and G.D. Shao, Electron force-induced dislocations annihilation and regeneration of a superalloy through electrical *in-situ* transmission electron microscopy observations, *J. Mater. Sci. Technol.*, 36(2020), p. 79.
[36] K. Chen, S.Y. Rui, F. Wang, J.X. Dong, and Z.H. Yao, Microstructure and homogenization process of as-cast GH4169D alloy for novel turbine disk, *Int. J. Miner. Metall. Mater.*, 26(2019), No. 7, p. 889.
[37] S.A. Sani, H. Arabi, S. Kheirandish, and G. Ebrahimi, Investigation on the homogenization treatment and element segregation on the microstructure of a γ/γ'-cobalt-based superalloy, *Int. J. Miner. Metall. Mater.*, 26(2019), No. 2, p. 222.
[38] Y.C. Liu, H.J. Zhang, Q.Y. Guo, X.S. Zhou, Z.Q. Ma, Y. Huang, and H.J. Li, Microstructure evolution of Inconel 718 superalloy during hot working and its recent development tendency, *Acta Metall. Sin.*, 54(2018), No. 11, p. 1653.
[39] D.L. Cui, X.Y. Xie, S.S. Li, H. Zhang, and S.K. Gong, Heat treatment of a Ni_3Al-based single crystal alloy IC32, *Mater. Sci. Forum*, 747-748(2013), p. 665.
[40] Z.G. Kong, L. Ji, S.S. Li, Y.F. Han, and H.B. Xu, Effect of heat treatment on microstructure and mechanical properties for a Ni_3Al base single crystal alloy DDIC6, *Mater. Sci. Forum*, 546-549(2007), p. 1443.
[41] E. Karakose and M. Keskin, Influences of high temperature on the microstructural, electrical and mechanical properties of Ni-23 wt.% Al alloy, *Int. J. Mater. Res.*, 106(2015), No. 1, p. 29.
[42] J. Lapin, Effect of ageing on the microstructure and mechanical behaviour of a directionally solidified Ni_3Al-based alloy, *Intermetallics*, 5(1997), No. 8, p. 615.
[43] D. Lee, Effects of solution heat treatment on the microstructure, oxidation, and mechanical properties of a cast Ni_3Al-based intermetallic alloy, *Met. Mater. Int.*, 12(2006), No. 2, p. 153.
[44] C. Ai, T.T. Zhai, M.Q. Ou, H. Zhang, L. Liu, S.S. Li, and S.K. Gong, Influence of heat treatment on microstructure of Ni_3Al based single crystal superalloy, *Mater. Res. Innov.*, 18(2014), Suppl. 4, p. 309.
[45] J. Wu, Y.C. Liu, C. Li, Y.T. Wu, X.C. Xia, and H.J. Li, Recent progress of microstructure evolution and performance of multiphase Ni_3Al-based intermetallic alloy with high Fe and Cr content, *Acta Metall. Sin.*, 56(2020), No. 1, p. 21.
[46] Y. Mishima, S. Ochiai, and T. Suzuki, Lattice parameters of

Ni(γ), Ni_3Al(γ′) and Ni_3Ga(γ′) solid solutions with additions of transition and B-subgroup elements, *Acta Metall.*, 33(1985), No. 6, p. 1161.

[47] F. Zhou, Y. Zhou, J. Wang, J.M. Liang, H.Y. Gao, and M.D. Kang, Enlightening from γ, γ′ and β phase transformations in Al–Co–Ni alloy system: A review, *Curr. Opin. Solid State Mater. Sci.*, 23(2019), No. 6, art. No. 100784.

[48] W. Gale, and Z.M. Abdo, Cast, and aged β-NiAl-β′-Ni_2AlTi-γ′-Ni_3Al-α-Cr alloys: A microstructural and mechanical properties investigation, *J. Mater. Sci.*, 34(1999), No. 18, p. 4425.

[49] C.T. Liu, W. Jemian, H. Inouye, J.V. Cathcart, S.A. David, J.A. Horton, and M.L. Santella, *Initial Development of Nickel and Nickel-Iron Aluminides for Structural Uses*, Report ORNL-6067, Oak Ridge National Laboratory, Tennessee, 1984.

[50] R. Yang, J.A. Leake, and R.W. Cahn, Chromium precipitation from β-Ni(Al, Ti) and γ'-Ni_3(Al, Ti) in the alloy $(Ni_{70}Al_{20}Ti_{10})_{0.9}Cr_{0.1}$, *Philos. Mag. A*, 65(1992), No. 4, p. 961.

[51] C.T. Liu and V.K. Sikka, Nickel aluminides for structural use, *JOM*, 38(1986), No. 5, p. 19.

[52] P. Pérez, P. González, G. Garcés, G. Caruana, and P. Adeva, Microstructure and mechanical properties of a rapidly solidified Ni_3Al–Cr alloy after thermal treatments, *J. Alloys Compd.*, 302(2000), No. 1-2, p. 137.

[53] J. Wu, C. Li, Y.C. Liu, Y.T. Wu, Q.Y. Guo, H.J. Li, and H.P. Wang, Effect of annealing treatment on microstructure evolution and creep behavior of a multiphase Ni_3Al-based superalloy, *Mater. Sci. Eng. A*, 743(2019), p. 623.

[54] J.Q. Li, Y.Y. Peng, J.B. Zhang, S. Jiang, S.P. Yin, J. Ding, Y.T. Wu, J. Wu, X.Q. Chen, X.C. Xia, X. He, and Y.C. Liu, Cyclic oxidation behavior of Ni_3Al-based superalloy, *Vacuum*, 169(2019), art. No. 108938.

[55] P. Subramani and M. Manikandan, Development of gas tungsten arc welding using current pulsing technique to preclude chromium carbide precipitation in aerospace-grade alloy 80A, *Int. J. Miner. Metall. Mater.*, 26(2019), No. 2, p. 210.

[56] Y.G. Zhang, Y.F. Han, and M.C. Chaturvedi, TEM studies of ETA carbide precipitate particles in a DS cast Ni_3Al base superalloy, *Mater. Charact.*, 34(1995), No. 3, p. 205.

[57] X.E. Zhang, H.L. Luo, S.P. Li, X. Cao, and S.Q. Li, Effection of alloying elements on microstructures of MX246 and MX246A Ni_3Al-based alloys, *J. Iron Steel Res. Int.*, 14(2007), No. 5, p. 45.

[58] R.N. Wright and J.R.Knibloe, The influence of alloying on the microstructure and mechanical properties of P/M Ni_3Al, *Acta Metall. Mater.*, 38(1990), No. 10, p. 1993.

[59] H. Li, J.T. Guo, M.H. Tan, C. Sun, W.H. Lai, and S.H. Wang, Microstructure and mechanical properties of Ni_3Al–Fe based alloy, *Acta Metall. Sin. Engl. Ed.*, 6(1993), No. 1, p. 40.

[60] C. Ai, S.S. Li, H. Zhang, L. Liu, Y. Ma, Y.L. Pei, and S.K. Gong, Effect of withdrawal rate on microstructure and lattice misfit of a Ni_3Al based single crystal superalloy, *J. Alloys Compd.*, 592(2014), p. 164.

[61] P. Li, S.S. Li, and Y.F Han, Influence of solution heat treatment on microstructure and stress rupture properties of a Ni_3Al base single crystal superalloy IC6SX, *Intermetallics*, 19(2011), No. 2, p. 182.

[62] J.T. Wang, H.L. Luo, S.P. Li, and X. Cao, Effect of solution treatment on stress rupture property of MX246A alloy, *Mater. Heat Treat.*, 39(2010), No. 12, p. 155.

[63] C. Ai, M.Q. Ou, X.B. Zhao, Y.L. Pei, H. Zhang, L. Liu, S.S. Li, and S.K. Gong, Effect of heat treatment and long-term age on microstructure of a Ni_3Al-based single crystal superalloy, *Mater. Res. Innov.*, 19(2015), Suppl. 4, p. S209.

[64] J.B. Singh, A. Verma, M.K. Thota, and J.K. Chakravartty, Brittle failure of Alloy 693 at elevated temperatures, *Mater. Sci. Eng. A*, 616(2014), p. 88.

[65] Y.F. Li, C. Li, J. Wu, Y.T. Wu, Z.Q. Ma, L.M. Yu, H.J. Li, and Y.C. Liu, Formation of multiply twinned martensite plates in rapidly solidified Ni_3Al-based superalloys, *Mater. Lett.*, 250(2019), p. 147.

[66] J. Wu, C. Li, Y.C. Liu, X.C. Xia, Y.T. Wu, Z.Q. Ma, and H.P. Wang, Influences of solution cooling rate on microstructural evolution of a multiphase Ni_3Al-based intermetallic alloy, *Intermetallics*, 109(2019), p. 48.

[67] Y.F. Feng, X.M. Zhou, J.W. Zou, and G.F. Tian, Effect of cooling rate during quenching on the microstructure and creep property of nickel-based superalloy FGH96, *Int. J. Miner. Metall. Mater.*, 26(2019), No. 4, p. 493.

[68] H.Q. Feng, Z.B. Yang, Y.T. Bai, L. Zhang, and Y.L. Liu, Effect of Cr content and cooling rate on the primary phase of Al-2.5Mn alloy, *Int. J. Miner. Metall. Mater.*, 26(2019), No. 12, p. 1551.

[69] Y.F. Li, C. Li, Y.T. Wu, J. Wu, Z.Q. Ma, H.J. Li, and Y.C. Liu, Microstructural evolution and phase transformation of Ni_3Al-based superalloys after thermal exposure, *Vacuum*, 171(2020), art. No. 109038.

[70] Y.F. Li, C. Li, J. Wu, H.J. Li, Y.C. Liu, and H.P. Wang, Microstructural feature and evolution of rapidly solidified Ni_3Al-based superalloys, *Acta Metall. Sin. Engl. Lett.*, 32(2019), No. 6, p. 764.

[71] X.T. Duan, S.P. Li, H.L. Luo, and J.T. Wang, Heat treatment process for Ni_3Al-based wrought superalloy, *J. Iron Steel Res.*, 27(2015), No. 11, p. 60.

[72] M. Hadi and A.R. Kamali, Investigation on hot workability and mechanical properties of modified IC-221M alloy, *J. Alloys Compd.*, 485(2009), No. 1-2, p. 204.

[73] A.M. Jokisaari, S.S. Naghavi, C. Wolverton, P.W. Voorhees, and O.G. Heinonen, Predicting the morphologies of γ′ precipitates in cobalt-based superalloys, *Acta Mater.*, 141(2017), p. 273.

[74] F. Masoumi, M. Jahazi, D. Shahriari, and J. Cormier, Coarsening and dissolution of γ′ precipitates during solution treatment of AD730™ Ni-based superalloy: Mechanisms and kinetics models, *J. Alloys Compd.*, 658(2016), p. 981.

[75] M.T. Kim, D.S. Kim, and O.Y. Oh, Effect of γ' precipitation during hot isostatic pressing on the mechanical property of a nickel-based superalloy, *Mater. Sci. Eng. A*, 480(2008), No. 1-2, p. 218.

[76] F. Liu and G.C. Yang, Effect of microstructure and γ′ precipitate from undercooled DD3 superalloy on mechanical properties, *J. Mater. Sci.*, 37(2002), No. 13, p. 2713.

[77] Z. Qiao, C. Li, H.J. Zhang, H.Y. Liang, Y.C. Liu, and Y. Zhang, Evaluation on elevated-temperature stability of modified 718-type alloys with varied phase configurations, *Int. J. Miner. Metall. Mater.*, 27(2020), No. 8, p. 1123.

[78] R.C. Reed, *The Superalloys: Fundamentals and Applications*, Cambridge University Press, Cambridge, 2006.

[79] J. Wu, C. Li, Y.C. Liu, X.C. Xia, Z.X. Zheng, and H.P. Wang, Precipitation of intersected plate-like γ′ phase in β and its effect on creep behavior of multiphase Ni_3Al-based intermetallic alloy, *Mater. Sci. Eng. A*, 767(2019), art. No. 138439.

[80] D. Lee, M.L. Santella, I.M. Anderson, and G.M. Pharr, Thermal aging effects on the microstructure and short-term oxidation behavior of a cast Ni_3Al alloy, *Intermetallics*, 13(2005), No. 2, p. 187.

[81] Q.Y. Li, S.Q. Tian, H.C. Yu, N. Tian, Y. Su, and Y. Li, Effects

of carbides and its evolution on creep properties of a directionally solidified nickel-based superalloy, *Mater. Sci. Eng. A*, 633(2015), p. 20.

[82] X.M. Dong, X.L. Zhang, K. Du, Y.Z. Zhou, T. Jin, and H.Q. Ye, Microstructure of Carbides at Grain Boundaries in Nickel Based Superalloys, *J. Mater. Sci. Technol.*, 28(2012), No. 11, p. 1031.

[83] X.C. Xia, Y.Y. Peng, J. Ding, C. Li, J.B. Zhang, X.G. Chen, X. He, S.P. Yin, and Y.C. Liu, Precipitation and growth behavior of gamma prime phase in Ni_3Al-based superalloy under thermal exposure, *J. Mater. Sci.*, 54(2019), No. 20, p. 13368.

[84] D.Y. Lee, An investigation of thermal aging effects on the mechanical properties of a Ni_3Al-based alloy by nanoindentation, *J. Alloys Compd.*, 480(2009), No. 2, p. 347.

[85] C.J. Li, G. Guo, Z.J. Yuan, W.D. Xuan, X. Li, Y.B. Zhong, and Z.M. Ren, Chemical segregation and coarsening of γ′ precipitates in Ni-based superalloy during heat treatment in alternating magnetic field, *J. Alloys Compd.*, 720(2017), p. 272.

[86] H.B. Motejadded, M. Soltanieh, and S. Rastegari, Coarsening kinetics of γ' precipitates in dendritic regions of a Ni_3Al base alloy, *J. Mater. Sci. Technol.*, 28(2012), No. 3, p. 221.

[87] X.C. Wu, Y.S. Li, W. Liu, Z.Y. Hou, and M.Q. Huang, Dynamics evolution of γ′ precipitates size and composition interface between γ/γ′ phases in Ni–Al alloy at different aging temperatures, *Rare Met.*, (2016), p. 1.

[88] L. Pichon, J.B. Dubois, S. Chollet, F. Larek, J. Cormie, and C. Templier, Low temperature nitriding behaviour of Ni_3Al-like γ′ precipitates in nickel-based superalloys, *J. Alloys Compd.*, 771(2019), p. 176.

[89] M. Li, J.X. Song, S.S. Li, and Y.F. Han, Effects of long-term aging at 1070°C on microstructure of Ni_3Al-base single-crystal alloy IC6SX, *Rare Met.*, 30(2011), p. 345.

[90] J. Wu, C. Li, Y.C. Liu, Y.T. Wu, X.C. Xia, Y.F. Li, and H.P. Wang, Formation and widening mechanisms of envelope structure and its effect on creep behavior of a multiphase Ni_3Al-based intermetallic alloy, *Mater. Sci. Eng. A*, 763(2019), art. No. 138158.

[91] Y.T. Wu, Y.C. Liu, C. Li, X.C. Xia, J. Wu, and H.J. Li, Coarsening behavior of γ′ precipitates in the γ′-γ area of a Ni_3Al-based alloy, *J. Alloys Compd.*, 771(2019), p. 526.

[92] J. Lapin and A. Vaňo, Coarsening kinetics of α- and γ′-precipitates in a multiphase intermetallic Ni–Al–Cr–Ti type alloy with additions of Mo and Zr, *Scripta Mater.*, 50(2004), No. 5, p. 571.

[93] J. Lapin, T. Pelachová, and O. Bajana, Microstructure and mechanical properties of a directionally solidified and aged intermetallic Ni–Al–Cr–Ti alloy with β-γ′-γ-α structure, *Intermetallics*, 8(2000), No. 12, p. 1417.

[94] D. Lee and M.L. Santella, Thermal aging effects on the mechanical properties of as-cast Ni_3Al-based alloy, *Mater. Sci. Eng. A*, 428(2006), No. 1-2, p. 196.

[95] Y.F. Han, S.H. Li, Y. Jin, and M.C. Chaturvedi, Effect of 900–1150 °C aging on the microstructure and mechanical properties of a DS casting Ni_3Al-base alloy IC6, *Mater. Sci. Eng. A*, 192-193(1995), p. 899.

[96] Y.T. Wu, Y.C. Liu, C. Li, X.C. Xia, J. Wu, and H.J. Li, Effect of initial microstructure on the hot deformation behavior of a Ni_3Al-based alloy, *Intermetallics*, 113(2019), art. No. 106584.